Electromagnetic line solitons in ferromagnets: suppression of a background instability

2008 J. Phys. A: Math. Theor. 41 185201

(http://iopscience.iop.org/1751-8121/41/18/185201)

IOP PUBLISHING JOURNAL OF PHYSICS A: MATHEMATICAL AND THEORETICAL

J. Phys. A: Math. Theor. **41** (2008) 185201 (12 pp) doi:10.1088/1751-8113/41/18/185201

Electromagnetic line solitons in ferromagnets: suppression of a background instability

H Leblond[1] **and M Manna**[2]

[1] Laboratoire POMA, CNRS-FRE 2988, Université d'Angers, 2 Bd Lavoisier, 49045 Angers Cedex 1, France
[2] Laboratoire de Physique Théorique et Astroparticules, CNRS-UMR 5207, Université Montpellier II, 34095 Montpellier, France

Received 10 December 2007, in final form 18 March 2008
Published 18 April 2008
Online at stacks.iop.org/JPhysA/41/185201

Abstract

The equations governing the propagation of polariton short solitary waves in a ferromagnetic slab are derived by means of a multiscale scheme. The effect of damping on the line solitons is discussed. A background instability occurs. Analysis shows that it can be suppressed by narrowing the slab in which the wave propagates.

PACS numbers: 41.20.Jb, 75.30.Ds, 02.30.Ik, 78.20.Bh

(Some figures in this article are in colour only in the electronic version)

1. Introduction

Bulk magnetic polaritons have been observed, mainly in antiferromagnets [1–3], in the linear regime. The linear theory has been developed [2, 4, 5]. However, the magnetic matter–wave interaction is intrinsically nonlinear. The propagation of solitons formed of polaritons in ferromagnets has been considered. The first studies were devoted to the slowly varying envelope approximation [6, 7]. The ferromagnetic case has also been investigated [8]. The long-wave approximation allowed us to describe the propagation of solitary waves, and of KdV (Korteweg–de Vries) solitons [9–11]. More recently short waves have been considered [12–14]. The latter structures have sizes much more relevant to available experiments than the former ones.

The short-wave approximation accounts in particular for the propagation of line solitons. It has been shown that these structures were stable for certain values of the soliton parameter [13]. However, two problems arise. First, the model derived in [13] neglects both the damping and the demagnetizing field, which are of importance in real ferromagnets. Second, numerical simulations of the stable line soliton reveal an instability of the constant background. The aim of the present paper is first to derive a more accurate model including damping and demagnetizing fields, and second to explain the background instability and to propose a way of re-stabilizing of the wave.

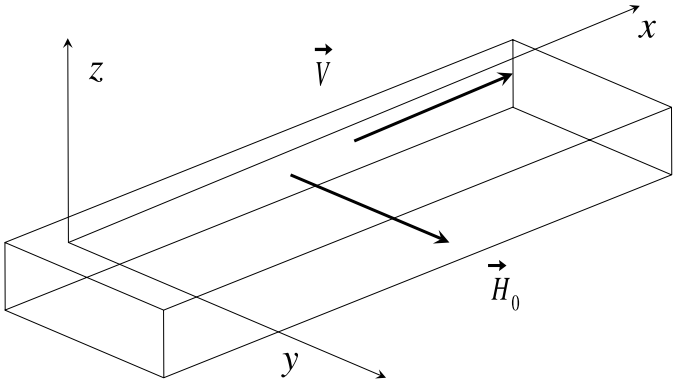

Figure 1. The configuration considered.

2. A (2+1)-dimensional generalization of the sine-Gordon equation

2.1. Basic equations

The evolution of the magnetic field **H** is governed by the Maxwell equations, which reduce to

$$-\nabla(\nabla\cdot\mathbf{H})+\Delta\mathbf{H}=\frac{1}{c^2}\partial_t^2(\mathbf{H}+\mathbf{M}), \tag{1}$$

where $c=1/\sqrt{\mu_0\tilde{\varepsilon}}$ is the speed of light with $\tilde{\varepsilon}$ being the scalar permittivity of the medium. The magnetization density **M** obeys the Landau–Lifschitz equation, which reads as

$$\partial_t\mathbf{M}=-\gamma\mu_0\mathbf{M}\wedge\mathbf{H}_{\text{eff}}+\frac{\sigma}{M_s}\mathbf{M}\wedge(\mathbf{M}\wedge\mathbf{H}_{\text{eff}}), \tag{2}$$

where γ is the gyromagnetic ratio, μ_0 is the magnetic permeability of the vacuum, σ is the damping constant and M_s is the saturation magnetization. The effective magnetic field is $\mathbf{H}_{\text{eff}}=\mathbf{H}-N\cdot\mathbf{M}$, where N is the demagnetizing factor tensor. We consider a ferromagnetic film lying in the xy plane, so that N is diagonal with $(N_x, N_y, N_z)=(0,0,1)$. The configuration is shown in figure 1.

We consider volume polaritons, in this case the wavelengths are large with regard to the exchange length. The typical wavelengths considered here are in the range of 10–100 μm. According to these assumptions, inhomogeneous exchange can be neglected, and the pinning boundary conditions are not to be considered. The slab thickness is assumed to be large with respect to the wavelength, say typically about 0.5 mm. This justifies that the exact boundary conditions are replaced by a mere demagnetizing tensor, and not taken into account, which would be necessary if we would consider surface modes or volume modes in thin films, but is not required here. We also assume that the crystalline and surface anisotropy of the sample can be neglected. The quantities **M**, **H** and t are rescaled into $\mu_0\gamma\mathbf{M}/c$, $\mu_0\gamma\mathbf{H}/c$ and ct, so that the constants $\mu_0\gamma/c$ and c in equations (2) and (1) are replaced by 1, M_s by $m=\mu_0\gamma M_s/c$ and σ by $\tilde{\sigma}=\sigma/\mu_0\gamma$, which is dimensionless.

The sample is supposed to be magnetized to saturation by means of an external uniform field, according to

$$\mathbf{M}_0=(m\cos\varphi, m\sin\varphi, 0), \qquad \mathbf{H}_0=\alpha\mathbf{M}_0. \tag{3}$$

The static field $\mathbf{H}_0$ lies in the plane xy, which is the plane of the film, and is thus collinear to the magnetization $\mathbf{M}_0$. The dispersion relation of linear waves propagating over this steady

state is, if the damping is neglected (this approximation is justified below),

$$\omega^2(\omega^2 - \mathbf{k}^2)^2 + m^2[(2+\alpha)\omega^2 - (1+\alpha)\mathbf{k}^2] \times [(k_y \cos\varphi - k_x \sin\varphi)^2 - (1+\alpha)\omega^2 + \alpha\mathbf{k}^2] = 0, \tag{4}$$

where α is the ratio of the applied field to the saturation magnetization, cf equation (3). It compares to the one derived in bulk media [13]. The coefficients $(1+\alpha)$ and α in the second parentheses become $(2+\alpha)$ and $(1+\alpha)$ respectively when the demagnetizing field is taken into account. Recall that the short-wave approximation is possible when the dispersion relation admits an expansion of the form [15, 16]

$$\omega = \frac{a}{\varepsilon} + b\varepsilon + c\varepsilon^3 + d\varepsilon^5 + \cdots, \tag{5}$$

where the small parameter ε is linked to the magnitude of the wavelength through $k_x = k_0/\varepsilon$, which corresponds to short waves. As in [13], where demagnetizing field was neglected, computation of the coefficients a, b, c, d shows that the expansion exists when $\varphi = \pi/2$ only. Thus the short-wave approximation is possible when the propagation direction x is perpendicular to the magnetization density, i.e. the short-wave soliton can propagate in a direction close to the perpendicular to the magnetization density only.

The direction of the wave propagation is assumed to be close to the x-axis, in such a way that the y variable gives only account of a slow transverse deviation. Therefore k_y is assumed to be very small with respect to k_x and we write $k_y = l_0$, of order 0 with respect to ε. The phase up to order ε is thus

$$\frac{1}{\varepsilon}(k_0 x - at) + l_0 y - \varepsilon b t, \tag{6}$$

which motivates the introduction of new variables

$$\zeta = \frac{1}{\varepsilon}(x - Vt), \qquad y = y, \qquad \tau = \varepsilon t. \tag{7}$$

The variable ζ allows us to describe the shape of the wave propagating with speed V, it assumes a short wavelength about $1/\varepsilon$. The slow time variable τ accounts for the propagation at very long time, on distances very large with regard to the wavelength. The transverse variable y has an intermediate scale, as in KP (Kadomtsev–Petviashvili)-type expansions [17].

Let us consider a slab with width about 0.5 cm. The slab width will play the role of the reference length. Taking the value of the perturbative parameter as $\varepsilon = 1/100$, it yields a length of the solitary wave in the range of 50 μm or less, and propagation distances which could in principle reach the meter, but are limited in practice to a few centimeter. The slab thickness is assumed to have an intermediary scale between the wavelength and the width, say about 0.5 mm.

2.2. The short-wave approximation

Let us now turn to the nonlinear aspect. Equation (7) allows us to introduce rescaled space and time operators, as

$$\frac{\partial}{\partial x} = \frac{1}{\varepsilon}\frac{\partial}{\partial \zeta}, \qquad \frac{\partial}{\partial y} = \frac{\partial}{\partial y}, \qquad \frac{\partial}{\partial t} = \frac{-V}{\varepsilon}\frac{\partial}{\partial \zeta} + \varepsilon\frac{\partial}{\partial \tau}. \tag{8}$$

The fields $\mathbf{M}$ and $\mathbf{H}$ are expanded in power series of ε, as

$$\mathbf{M} = \mathbf{M}_0 + \varepsilon\mathbf{M}_1 + \varepsilon^2\mathbf{M}_2 + \cdots, \tag{9}$$

$$\mathbf{H} = \mathbf{H}_0 + \varepsilon\mathbf{H}_1 + \varepsilon^2\mathbf{H}_2 + \cdots, \tag{10}$$

where $\mathbf{M}_0, \mathbf{H}_0, \mathbf{M}_1, \mathbf{H}_1, \ldots$ are functions of (ζ, y, τ), and analogously for $\mathbf{H}$. The boundary conditions are

$$\lim_{\zeta \longrightarrow -\infty} \mathbf{H}_j = \lim_{\zeta \longrightarrow -\infty} \mathbf{M}_j = \mathbf{0}, \tag{11}$$

for all $j \geqslant 1$, and

$$\lim_{\zeta \longrightarrow -\infty} \mathbf{H}_0 = \alpha \lim_{\zeta \longrightarrow -\infty} \mathbf{M}_0 = \alpha(0, m, 0). \tag{12}$$

We further assume that the damping is weak. In yttrium-iron-garnet (YIG) films, envelope solitons have been observed [18, 19]. It has been shown that the observations could be accounted for using a NLS-type model including the damping term. Such a model can be derived for the Landau–Lifschitz and Maxwell equations (2) and (1), assuming that the dimensionless damping constant $\tilde{\sigma}$ is small, of order ε^2 where ε is a perturbative parameter measuring the amplitude of the magnetic wave pulse [20]. In YIG films, $\tilde{\sigma}$ can be as small as 10^{-4} [21], which would correspond to a perturbative parameter $\varepsilon \simeq 0.01$. We will show below that under this assumption, the effect of the damping can be completely neglected within the short-wave approximation. In order to be able both to justify this statement and to derive an equation which takes into account a stronger damping, we set $\tilde{\sigma} = \varepsilon^p \bar{\sigma}$. The value $p = 2$ holds for a YIG film with low losses, and $p = 1$ in other cases. Let us first assume that $p = 1$.

Expansions (9), (10) and operators (8) are reported into equations (2) and (1), and solved order by order. At leading order $1/\varepsilon^2$, as in the bulk medium, is found that $\mathbf{M}_0$ is uniform, that $H_0^x = 0$, and that the velocity is $V = 1$, i.e., in physical units, the speed c of light in the medium. At order $1/\varepsilon$, we get expressions of $\mathbf{M}_1$ and H_1^x identical to those obtained in [13]. At order ε^0, the damping appears in equation (2), which yields

$$\partial_\zeta \mathbf{M}_2 = \begin{pmatrix} m H_1^z \\ -M_1^x H_0^z \\ -m H_1^x + M_1^x H_0^y + \bar{\sigma} m H_0^z \end{pmatrix}. \tag{13}$$

Then, making use of (13) into equation (1), we get the conditions

$$-\partial_y H_1^x + 2\partial_\tau H_0^y + M_1^x H_0^z = 0, \tag{14}$$

as in the bulk, and

$$\partial_y^2 H_0^z + 2\partial_\zeta \partial_\tau H_0^z + m\partial_\zeta H_1^x - \partial_\zeta \left(M_1^x H_0^y\right) - \bar{\sigma} m \partial_\zeta H_0^z = 0, \tag{15}$$

which, in addition, includes the damping term $-\bar{\sigma} m \partial_\zeta H_0^z$. Using the relations obtained at previous orders, equations (14) and (15) reduce to

$$\int_{-\infty}^{\zeta} \partial_y^2 H_0^y \, \mathrm{d}\zeta' + \partial_y M_1^x + 2\partial_\tau H_0^y + \frac{1}{m} M_1^x \partial_\zeta M_1^x = 0, \tag{16}$$

$$\frac{-1}{m} \partial_y^2 \partial_\zeta M_1^x - \frac{2}{m} \partial_\zeta^2 \partial_\tau M_1^x + m\partial_y H_0^y + m\partial_\zeta M_1^x + \partial_\zeta \left(M_1^x H_0^y\right) + \bar{\sigma} \partial_\zeta^2 M_1^x = 0. \tag{17}$$

Equations (16) and (17) yield the sought asymptotic model.

2.3. The nonlinear equations

Only equation (17) contains a damping term. Furthermore, it has been derived under the assumption of a relatively strong damping $p = 1$. If we assume, as is reasonable in a YIG film, the assumption of small damping corresponding to $p = 2$, it is clear from the above calculation that the first correction due to the damping will appear at the next

order in the perturbative scheme only, and hence the asymptotic model obtained will not contain any damping term at all. It can be recovered setting $\bar{\sigma} = 0$ in equation (17). This differs from the case of envelopes, for which damped solitons were obtained under the same assumptions [20]. The discrepancy comes from the fact that the propagation distance is much smaller in the short-wave approximation ($\propto 1/\varepsilon$) than for the nonlinear envelope evolution ($\propto 1/\varepsilon^2$), while the distance characteristic of the damping is the same ($\propto 1/\varepsilon$).

If damping is neglected, system (16) and (17) exactly coincides with the system derived in [13], in which the demagnetizing factor was omitted. Hence, within the considered approximation, and for the geometry considered, the demagnetizing field has no effect on the wave propagation, which is rather remarkable. We check that the following terms in the perturbative expansion can be computed, which ensures the validity of the asymptotic.

Setting

$$A = \frac{-H_0^y}{m} - 1, \qquad B = \frac{M_1^x}{2m}, \tag{18}$$

$$X = \frac{-m}{2}\zeta, \qquad Y = my, \qquad T = m\tau, \tag{19}$$

$$s = \frac{-\bar{\sigma}}{2}, \tag{20}$$

reduces equations (16) and (17) to

$$\partial_X \partial_T B = AB + \partial_Y^2 B - \int^X \partial_Y A - s\partial_X B, \tag{21}$$

$$\partial_X \partial_T A = -\partial_X (B\partial_X B) + \partial_Y^2 A + \partial_X \partial_Y B, \tag{22}$$

where $\int^X f$ denotes a primitive of f vanishing as $X \longrightarrow +\infty$. Note that $\sigma < 0$ and hence $s > 0$.

Some symmetry is recovered in the system by setting

$$A = \partial_X C, \tag{23}$$

which reduces system (21), (22) to

$$C_{XT} = -BB_X + C_{YY} + B_Y, \tag{24}$$

$$B_{XT} = BC_X + B_{YY} - C_Y - sB_X, \tag{25}$$

where the subscripts denote partial derivatives (i.e. $C_Y = \partial_Y C$, and so on).

2.4. The line soliton

Assume now that the damping is small according to $\tilde{\sigma} = \varepsilon^2 \bar{\sigma}$, which is valid e.g. in YIG. Then the damping is negligible, and the demagnetizing field has no effect. Hence the results established in bulk media [13] apply.

In (1+1) dimensions, setting

$$B_X = A\sin\theta, \qquad C_X = \sin\theta, \tag{26}$$

the system (24), (25) reduces to

$$\theta_{XT} = A\sin\theta, \tag{27}$$

A being a constant. Equation (27) is the sine-Gordon equation, which is completely integrable by means of the inverse scattering transform method [22, 23], and was first derived in the frame of electromagnetic waves in ferromagnets in [12]. It admits the kink solution

$$B = 2w \operatorname{sech} \zeta, \qquad C = w(2 \tanh \zeta - \zeta), \qquad \zeta = (X - wT), \tag{28}$$

where the velocity w of the kink is an arbitrary real parameter. Solution (28) to (27) obviously yields a solution of system (24), (25) in the form of a line soliton: a solitary wave invariant in the transverse direction. A more general plane solitary wave can be deduced from solution (28), as

$$B = p + 2w \operatorname{sech} \zeta, \qquad C = w(2 \tanh \zeta - \zeta), \qquad \zeta = X + pY - (w - p^2)T, \tag{29}$$

where p is an arbitrary real parameter. For nonzero p, w does not represent the soliton velocity any more. The stability of the line soliton (28) with respect to slow transverse perturbations is studied in [13]. It is shown that the line soliton is stable if its velocity w is less than

$$w_{\text{th}} = \frac{\pi^2}{8} - 1, \tag{30}$$

and unstable for $w > w_{\text{th}}$. This has been confirmed by numerical analysis.

The various change of variables we used to derive (24), (25) contain a sign change with respect to x. Further the velocity w of the line soliton is a correction to wave speed with respect to the speed of light in the medium. Therefore, the stable line solitons, which have a negative velocity relative to the normalized variables, have a velocity larger than c. In some sense, they are 'supraluminous'. There is no contradiction in this fact, since the refractive index $\sqrt{\varepsilon_r}$ of the medium is very large, and the relative velocity w represents a small correction (of order ε^2). Hence the corrected velocity, although it is larger than c, will be smaller than the light velocity in vacuum c_0.

The numerical scheme used for solving the model without damping [13] is straightforwardly generalized to take the damping into account. Figures 2 and 3 show the effect of damping on a line soliton.

The initial data are perturbed, so that stability is evidenced. The box size is determined by $0 < x < 24, -40 < y < 40, 0 < t < 30$, the number of points is $(n_x, n_y, n_t) = (1000, 140, 24000)$. The soliton decay due to the damping is clearly seen. However, the damping of B (or H_0^z) is much slower than it would be in the linear case. The amplitude is indeed reduced from 0.4 to about 0.25, against $0.4\,\mathrm{e}^{-sT} = 0.15$ in the linear case. In contrast, C (i.e. H_0^y) is damped too, despite equation (24) contains no damping term. The damping of this component is hence due to the nonlinear interaction between the two components only. Numerical investigation shows that the damping has no other effect.

3. Suppression of a background instability

3.1. Instability

Even when the line soliton itself is stable, the numerical resolution of system (24), (25) shows some other kind of instability, which appears to be an instability of the transverse modulation of the background. An example is given in figure 4, corresponding to an initial background level w close to 0.

Oscillations in the Y-direction arise spontaneously. The wavelength can be determined using a fast Fourier transform. For example, it is about 13.4, which corresponds to a wavevector $q \simeq 0.47$. Note that this value becomes modified for larger values of X. This instability is not suppressed when damping is introduced, it occurs with the data of figures 2 and 3, for larger X and T.

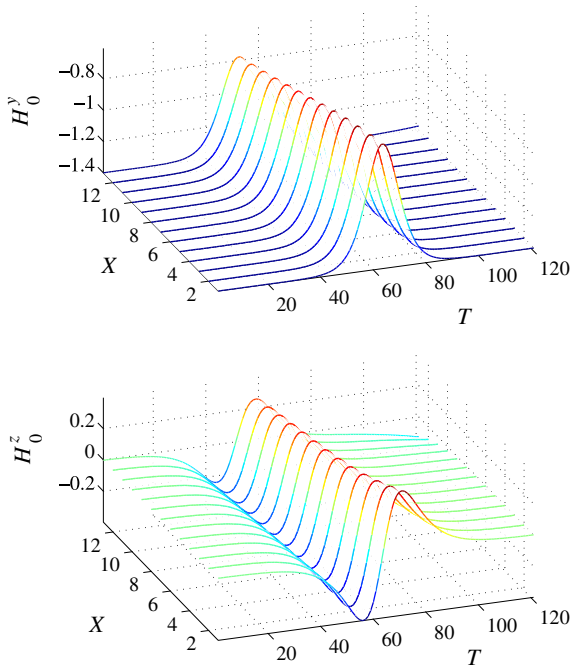

Figure 2. Time evolution of the longitudinal profile of the line soliton. The soliton parameter is $w = 0.4$ in the stable range. The normalized damping constant is $\bar{\sigma} = -0.4$.

This background is defined by a uniform value of the components H_0^y, H_0^z of the magnetic field, which are related to the dynamical variables B, C through

$$H_0^y = -m(1 + C_X), \qquad H_0^z = -mB_X. \tag{31}$$

The uniform background corresponds thus to solutions of the form $C = Xf$, $B = Xg$, where f and g are constants. Analysis of the modulation instability of these solutions consists in introducing a small harmonic variation of f and g relative to Y, and studying its evolution with the time T. A standard linear stability analysis would involve system (24), (25), linearized about the uniform background solution. Due to the particular dependence of system (24), (25) with respect to X and T, the coefficients of the linearized system depend on X, and the standard procedure cannot be used. Therefore we introduce a scaled time $\tau = XT$, and assume that

$$C = Xf(Y, \tau = XT), \tag{32}$$

$$B = Xg(Y, \tau = XT). \tag{33}$$

Expressions (32), (33) are reported into system (24), (25), and then a small time approximation is used: the terms proportional to $\tau = XT$ are neglected. We get the following equations:

$$2f_\tau = -g^2 + g_Y + f_{YY}, \tag{34}$$

$$2g_\tau = fg + g_{YY} - f_Y - \frac{s}{X}g. \tag{35}$$

The damping term is not independent of X, and even singular. Neglecting damping ($s = 0$) would allow us to avoid the difficulty. Looking for constant solutions $f = f_0$, $g = g_0$ of (35),

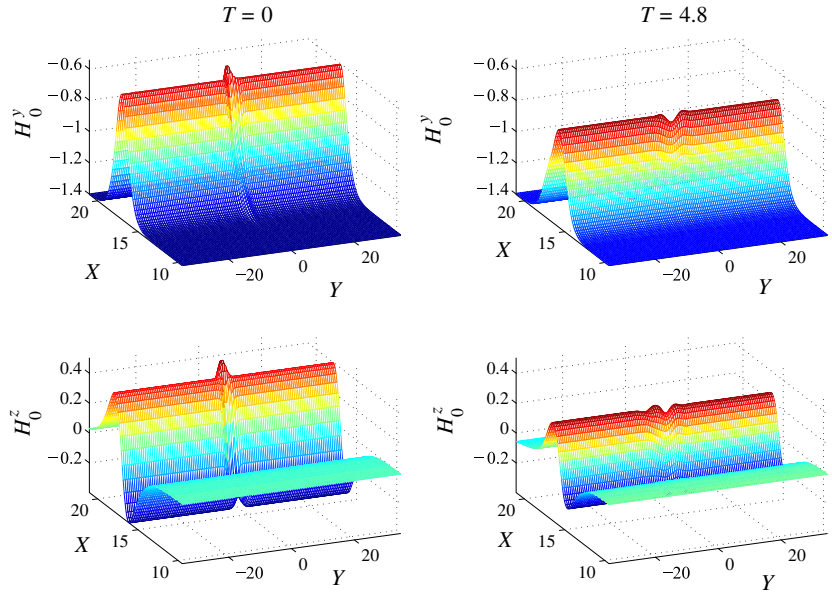

Figure 3. Evolution of a perturbed stable damped line soliton. Left: the initial state. Right: after a propagation time $T = 4.8$. The decrease of the soliton amplitude due to the damping, and the decrease of the perturbation amplitude due to the stability, are observed (same data as figure 2).

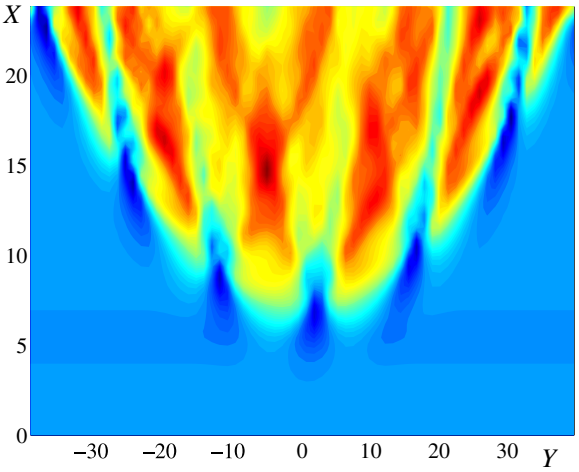

Figure 4. Background instability: oscillations in the Y-direction arise spontaneously. The initial data are a perturbed stable line soliton with velocity $w = 0.02$, the evolution time is $T = 22$, and damping is neglected ($\bar{\sigma} = 0$).

we see that g_0 must be zero while f_0 remains free. This is consistent with the kink solution (28) of system (24), (25) with no damping ($s = 0$). In the present limit it yields $C \simeq -wX$, and $B \simeq 0$. Therefore we set

$$f = -w + \gamma\, \mathrm{e}^{(\mathrm{i}qY + \lambda\tau)} + \cdots, \tag{36}$$

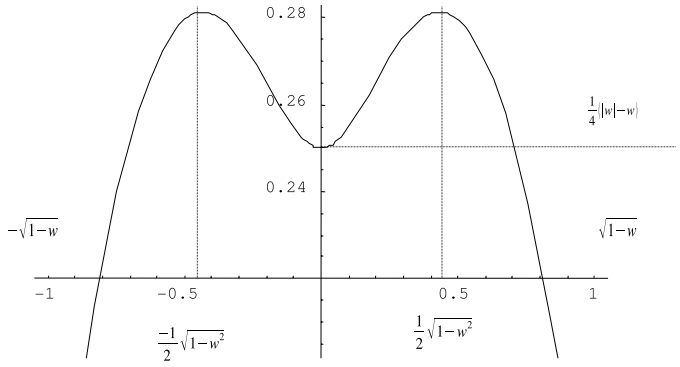

Figure 5. Plot of the growth rate λ against the transverse wave number q.

$$g = \beta\, \mathrm{e}^{(\mathrm{i}qY+\lambda\tau)} + \cdots. \tag{37}$$

Reporting (37) into equations (24) and (25), we find that the condition of existence of nonzero β, γ is

$$(2\lambda + q^2)(2\lambda + q^2 + \tilde{w}) = q^2, \tag{38}$$

where $\tilde{w} = w + s/X$. Let us denote by λ_1 and λ_2 the two solutions of equation (38). Figure 5 presents the largest of the two solutions λ_1 and λ_2 against q for $-1 < w < 0$ (precisely $\tilde{w} = -0.5$), which allows us to depict the general case.

Since $\lambda_1\lambda_2$ and $\lambda_1 + \lambda_2$ have the same sign as $(q^2 + \tilde{w} - 1)$ and $-(2q^2 + \tilde{w})$ respectively, it is seen that λ_1 and λ_2 are both negative for any real q if $\tilde{w} > 1$, while one of them is positive for $|q| < \sqrt{1-\tilde{w}}$ if $\tilde{w} < 1$. The maximum of λ_j is obtained for $q = \pm\frac{1}{2}\sqrt{1-w^2}$ when $-1 < w < 1$, and $q = 0$ when $w < -1$. It gives the wavelength of the transverse oscillations that arise spontaneously due to the instability. As an example, for a background level $w = 0$, the most unstable wavevectors are $q = \pm 1/2$, and the wavelength is $2\pi/q = 4\pi$, which is in good accordance with the numerical results of figure 4.

The conclusion is that the uniform background is stable when $\tilde{w} > 1$, while it is unstable when $\tilde{w} < 1$. In terms of the magnetic field, the background level w is $w = -C_X = 1 + H_0^y/m$, or in physical units $w = 1 + H_0^y/M_s$. Neglecting the damping, the stability condition $w > 1$ corresponds to a magnetization which has the same direction as the applied field, and it is well known that the opposite situation is unstable. Recall that the line soliton is stable if $w < \pi^2/8 - 1 \simeq 0.24$, which always belongs to the domain of unstable background.

Since $\tilde{w} > w$, the stability condition is less restrictive if damping is taken into account. Transverse stability is possible for a small H_0^y in the direction opposite to the magnetization, on a short distance.

3.2. Filtering

In the case of the unstable background, with the magnetic field and magnetization in opposite directions, the instability is due to the small wave numbers q, i.e. long wavelengths. If some filtering of the long wavelengths is introduced, the stability can be recovered. This can be done by limiting the width l of the sample, since the allowed wave numbers are at most $2\pi/l$. Thus the background is stabilized if

$$l < \frac{2\pi}{\sqrt{\tilde{w} - 1}}. \tag{39}$$

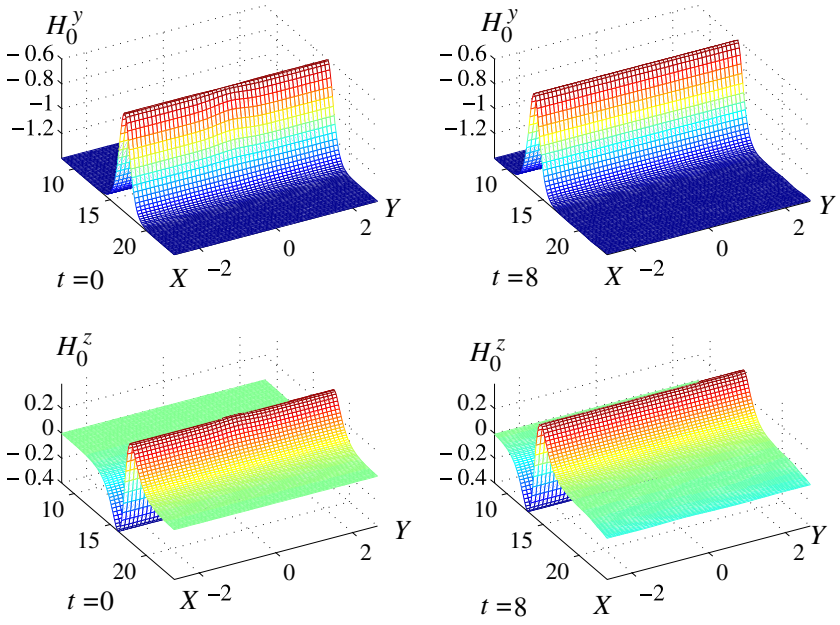

Figure 6. Stable propagation of an initially perturbed line soliton. The background is stabilized using the narrowing of the stripe where propagation occurs. The line-soliton velocity is $w = -0.4$, the evolution time is $T = 8$ and damping is neglected ($\bar{\sigma} = 0.$).

A numerical example and confirmation of this property is given in figure 6. The value $w = -0.4$ of the velocity corresponds to a stable line soliton but to an unstable background. The maximal width which is expected to eliminate the transverse instability of the background is $l = 2\pi/\sqrt{1.4} \simeq 5.31$, according to (39). The computation has been performed using $l = 5.30$, and periodic boundary conditions in the transverse direction. The instability is suppressed, which confirms numerically the above analysis.

The threshold width l can be computed according to condition (39) above, in physical units, it is

$$l = \frac{2\pi c}{\mu_0 \gamma \sqrt{-H_0^y M_s}}. \tag{40}$$

We consider typical values as $H_0 = 2$ kOe, M_s (or $4\pi M_s$) $= 1800$ Oe, $\gamma\mu_0 = 1.759 \times 10^7$ rad s^{-1} Oe^{-1}. The speed of light is $c = c_0/\sqrt{\varepsilon_r}$, where $c_0 = 3 \times 10^8$ m s^{-1}, and ε_r is the relative permittivity of the medium, for YIG we can take $\varepsilon_r = 12$, then $c = 8.66 \times 10^7$ m s^{-1}. We get $l \simeq 1.6$ cm. The length of the single-oscillation line soliton is 1 relative to the normalized variable X, which yields

$$x_0 = \frac{2\varepsilon c}{\gamma \mu_0 M_s}, \tag{41}$$

in physical units. It depends on the perturbative parameter ε and hence is adjustable in some range. For the above data, and taking $\varepsilon = 1/100$, we get $x_0 \simeq 50$ μm.

An analogous phenomenon of transverse stabilization of a wave depending on the film width has been experimentally observed in the case of spin wave envelope solitons in YIG films [24]. The authors observed stable propagation of a line soliton in a narrow stripe of width

1.5 mm, while the transverse self-focusing occurred in a wide film of 18 mm width. Thus the transverse instability of the wave is suppressed when the width of the film is decreased below some threshold which lies between 1.5 mm and 18 mm. The analogy, although not complete, is clear, and the thresholds for the width have the same order of magnitude. Note further that, in the experimental situation, the transverse modes to be considered are the guided mode of the stripe, and not pure Fourier modes as in the above theory. On this ground, it could be expected that the stability maximal width will be smaller in the experiment than the value predicted above. Indeed, numerical computation using free lateral boundary conditions instead of periodic ones shows the stabilization for a lower width only, and an analogous behavior is expected for the exact guiding conditions. Note however that the experimental result concerns a propagation mode, backward volume magnetostatic waves, which differs from the one considered in the present paper, and that the transverse instability considered in the experiment is that of the wave, while it concerns the background in the above theory.

4. Conclusion

The equations governing the evolution of a short solitary wave in a ferromagnetic slab have been derived. The wave belongs to the so-called electromagnetic or polariton range. The analysis shows that both demagnetizing field and damping can be neglected, at least in low-loss materials such as YIG. The effect of damping is only a decay of the soliton amplitude, and this decay is slower with respect to the corresponding linear regime.

A background instability has been observed in numerical simulations, it corresponds to a magnetization reversed with respect to the applied field. This instability can be suppressed if the slab is narrow enough. The threshold width for the stabilization, about 1.5 centimeters, falls in the range of sample widths currently used in experiments. If the unstable state where the magnetic field and magnetization have opposite directions perpendicular to the sample axis is realized, solitary waves can propagate along the slab without deformation, and the transverse instability is suppressed if the slab is narrow enough.

Acknowledgment

This work is made under contract CNRS GDR-PhoNoMi2 (Photonique Nonlinéaire et Milieux Microstructurés).

References

[1] Jensen M R F, Feiven S A, Parker T J and Camley R E 1997 Experimental observation and interpretation of magnetic polariton modes in FeF_2 *J. Phys.: Condens. Matter* **9** 7233–47
[2] Camleyn R E 1999 Magnetization dynamics in thin films and multilayers *J. Magn. Magn. Mater.* **200** 583–97
[3] Tarakanov V V, Khizhnyi V I, Korolyuk A P and Strugatsky M B 2000 Excitation of magnetic polaritons in plates of $FeBO_3$ *Physica* **284–288** 1452–3
[4] Arakelian V H, Bagdassarian L A and Simonian S G 1997 Electrodynamics of bulk and surface normal magnon-polaritons in antiferromagnetic crystals *J. Magn. Magn. Mater.* **167** 149–60
[5] Guimarães E S and Albuquerque E L 2002 Spin canted magnetic polaritons in thin films *Solid State Commun.* **122** 623–8
[6] Leblond H and Manna M 1994 Benjamin–Feir type instability in a saturated ferrite. Transition between a focusing and defocusing regimen for polarized electromagnetic wave *Phys. Rev.* E **50** 2275
[7] Leblond H 1999 Electromagnetic waves in ferromagnets: a Davey–Stewartson type model *J. Phys. A: Math. Gen.* **32** 7907–32
[8] Daniel M and Veerakumar V 2002 Propagation of electromagnetic soliton in antiferromagnetic medium *Phys. Lett.* **302** 77–86

[9] Leblond H 1995 Interaction of two solitary waves in a ferromagnet *J. Phys. A: Math. Gen.* **28** 3763–84
[10] Leblond H 2002 KP lumps in ferromagnets: a three-dimensional KdV–Burgers model *J. Phys. A: Math. Gen.* **35** 10149–61
[11] Leblond H 2003 A new criterion for the existence of KdV solitons in ferromagnets *J. Phys. A: Math. Gen.* **36** 1855–68
[12] Kraenkel R A, Manna M A and Merle V 2000 Nonlinear short-wave propagation in ferrites *Phys. Rev.* E **61** 976–9
[13] Manna M and Leblond H 2006 Transverse stability of short line-solitons in ferromagnetic media *J. Phys. A: Math. Gen.* **39** 10437–47
[14] Leblond H and Manna M 2007 Single-oscillation two-dimensional solitons of magnetic polaritons *Phys. Rev. Lett.* **99** 064102
[15] Manna M A and Merle V 1998 Asymptotic dynamics of short waves in nonlinear dispersive models *Phys. Rev.* E **57** 6206
[16] Manna M A 2001 Nonlinear asymptotic short-wave models in uid dynamics *J. Phys. A: Math. Gen.* **34** 4475
[17] Kadomtsev B B and Petviashvili V I 1970 On the stability of solitary waves in weakly dispersing media *Sov. Phys.—Dokl.* **15** 539–41
[18] De Gasperis P, Marcelli R and Miccoli G 1987 Magnetostatic soliton propagation at microwave frequency in magnetic garnet films. *Phys. Rev. Lett.* **59** 481
[19] Slavin A N and Rojdestvenski I V 1994 'Bright' and 'dark' spin wave envelope solitons in magnetic films *IEEE Trans. Magn.* **30** 37
[20] Leblond H 1996 Electromagnetic waves in ferrites: from linear absorption to the nonlinear Schrödinger equation *J. Phys. A: Math. Gen.* **29** 4623–39
[21] Lecraw R C, Spencer E G and Porter C S 1958 Ferromagnetic resonance line width in yttrium iron garnet single crystals *Phys. Rev.* **110** 1311
[22] Ablowitz M J and Segur H 1981 *Solitons and the Inverse Scattering Transform* (Philadelphia, PA: SIAM)
[23] Dodd R K, Eilbeck J C, Gibbon J D and Morris H C 1982 *Solitons and nonlinear wave equations* (London: Academic)
[24] Büttner O, Bauer M, Demokritov S O, Hillebrands B, Kostylev M P, Kalinikos B A and Slavin A N 1999 Collisions of spin wave envelope solitons and self-focused spin-wave packets in yttrium iron garnet films *Phys. Rev. Lett.* **82** 4320–3